STM JOURNALS

Journal of
Polymer & Composites

ISSN: 2321-2810 (Online)
ISSN: 2321-8525 (Print)
Volume 14, Special Issue 2, 2026
DOI (Journal): 10.37591/JoPC

https://journals.stmjournals.com/jopc

Research JoPC

Development and Performance Evaluation of Polymer-Modified Geopolymer Composites Incorporating GGBS

Mayuri Patil[1,*], Amit Kumar Ahirwar[2]

Abstract:

This research investigates the development and performance of geopolymer-based composite materials formulated using Ground Granulated Blast Furnace Slag (GGBS) as a reactive mineral component within an aluminosilicate polymer matrix. The study aims to create an eco-efficient and structurally sound inorganic polymer composite comparable to M35-grade concrete, produced entirely under ambient curing conditions. A series of mixes with varying GGBS replacement ratios (0–100%) was prepared, maintaining a constant binder content of 400 kg/m³ and an activator-to-binder ratio of 0.45. The polymerisation reaction between sodium hydroxide (NaOH) and sodium silicate (Na_2SiO_3) solutions facilitated the formation of a cross-linked aluminosilicate network, serving as a polymeric binder reinforced by calcium-rich GGBS particles. Mechanical testing, including compressive, flexural, and split tensile strength, as well as durability assessments such as water absorption and sorptivity, were conducted at 7, 14, and 28 days. Microstructural and spectroscopic analyses (FTIR, Raman, TGA/DTA, XRD) confirmed the development of a hybrid C–A–S–H/N–A–S–H composite gel structure, indicating strong interfacial bonding and matrix densification. The 28-day compressive strength increased from 28.8 MPa to 41.6 MPa with increasing GGBS content, while water absorption and sorptivity decreased by over 30%, demonstrating improved composite integrity and reduced permeability. The optimal mix (60–80% GGBS) delivered superior performance and sustainability, achieving nearly a 90% reduction in embodied carbon compared with OPC-based systems. Overall, this study advocates GGBS-based geopolymer concrete as a sustainable inorganic polymer composite that offers high mechanical performance, microstructural stability, and environmental compatibility for next-generation structural applications.

Keywords: Geopolymer composites, ground granulated blast furnace slag (GGBS), inorganic polymer matrix, alkali activation, C–A–S–H / N–A–S–H Gels, composite microstructure

INTRODUCTION

The global construction industry is shifting towards environmentally sustainable, high-performance materials, driven by rising demand for eco-friendly infrastructure and the need to reduce greenhouse gas emissions [1]. While Ordinary Portland Cement (OPC)-based systems remain common in structural engineering, their production consumes substantial energy and accounts for about 7–8% of worldwide CO_2 emissions [2]. This environmental impact calls for alternative binders with much lower embodied carbon and better durability. In this context, alkali-activated geopolymer binders have become promising options, functioning as inorganic polymers that form three-dimensional aluminosilicate networks, akin to polymer cross-linking [3, 4]. Geopolymers are a unique class of mineral-based polymer composites formed by

*Author for Correspondence
Mayuri Patil

[1]Research Scholar, Department of civil engineering, Rabindranath Tagore University, Bhopal, Madhya Pradesh, India
[2]Assistant Professor, Department of civil engineering, Rabindranath Tagore University, Bhopal, Madhya Pradesh, India

Received Date: November 10, 2025
Accepted Date: November 27, 2025
Published Date: April 22, 2026

Citation: Mayuri Patil, Amit Kumar Ahirwar. Development and Performance Evaluation of Polymer-Modified Geopolymer Composites Incorporating GGBS. Journal of Polymer & Composites. 2026; 14(Special Issue 2): S1145–S1165p.

reactions between aluminosilicate precursors and alkaline activators, yielding rigid binder phases such as sodium aluminosilicate hydrate (N–A–S–H) and calcium aluminosilicate hydrate (C–A–S–H) gels [5]. These polymeric gels offer excellent chemical bonding, lower porosity, and high thermal stability, providing greater resistance to harsh environments than traditional cementitious systems. Among the precursors, Ground Granulated Blast Furnace Slag (GGBS) is especially appealing due to its high calcium content, fine particle size, and latent hydraulic reactivity, which promote rapid polymerisation and early strength gain at room temperature [6]. The construction industry consumes large amounts of natural resources and significantly contributes to global greenhouse gas emissions, with cement production alone responsible for nearly 7–8% of global CO_2 emissions [7]. OPC, the main binder in concrete, is produced by calcining limestone and burning fossil fuels—processes that emit high levels of carbon and deplete finite raw materials [8]. Moreover, large-scale limestone and clay extraction cause environmental damage, and OPC-based concrete often struggles with durability in aggressive settings, leading to higher maintenance needs [9, 10]. As infrastructure demands increase, the environmental impact of traditional materials presents major challenges to sustainable growth [11]. This has led researchers and industry professionals to seek innovative, low-carbon binder systems that reduce environmental harm without sacrificing performance [12]. Geopolymer technology has emerged as a promising alternative [13]. Geopolymers are inorganic binders created via the alkali activation of aluminosilicate-rich materials like fly ash, metakaolin, and GGBS [13, 14]. During geopolymerization, silica (SiO_2) and alumina (Al_2O_3) dissolve in an alkaline solution and polycondense into a stable three-dimensional aluminosilicate network [15, 16]. Depending on the calcium content, the binding matrix mainly forms sodium aluminosilicate hydrate (N–A–S–H) gel or a combination of N–A–S–H and calcium aluminosilicate hydrate (C–A–S–H) gels—the latter typical of GGBS-based mixes [17, 18]. Compared to OPC hydration, geopolymers have much lower embodied carbon, higher early strength, better chemical resistance, less shrinkage, and improved performance at high temperatures [19]. GGBS is especially beneficial due to its latent hydraulic properties, high CaO content, and small particle size, which accelerate reactions and strengthen the geopolymer matrix [20, 21]. Using GGBS also supports circular economy principles, as it is a steel industry by-product that reduces landfill waste and decreases reliance on virgin raw materials [22, 23].

- To develop M35-grade geopolymer concrete mixes by partially and entirely replacing Ordinary Portland Cement (OPC) with Ground Granulated Blast Furnace Slag (GGBS) under ambient curing conditions.
- To evaluate the effect of varying GGBS replacement levels (0–100%) on the mechanical properties of geopolymer concrete, including compressive strength, flexural strength, and split tensile strength at 7, 14, and 28 days.
- To assess the influence of GGBS content on durability characteristics, specifically water absorption and sorptivity, and to establish the relationship between GGBS dosage and pore structure refinement.
- To perform microstructural and chemical analyses (FTIR, Raman Spectroscopy, TGA/DTA, and XRD) to identify gel phases (C–A–S–H and N–A–S–H) and understand how GGBS alters the geopolymerisation mechanism and matrix densification.
- To determine the optimal GGBS replacement level that balances mechanical strength, durability, and workability for sustainable M35-grade geopolymer concrete suitable for structural applications.
- To evaluate the sustainability performance of GGBS-based geopolymer concrete by quantifying reductions in embodied CO_2 emissions and promoting circular economy practices through the use of industrial by-products.
- To compare the performance of M35 geopolymer concrete with conventional OPC concrete and demonstrate its potential as a low-carbon, durable, and eco-efficient alternative for modern construction.

LITERATURE REVIEW

Growing interest in sustainable building materials has driven extensive worldwide research into

geopolymer technology as a low-carbon alternative to Ordinary Portland Cement (OPC). The early study by Davidovits (1991) introduced the concept of alkali-activated binders, demonstrating that aluminosilicate-rich wastes could undergo polymeric transformation under alkaline conditions to form high-strength, durable matrices [24–25]. Subsequent research (Duxson et al., 2007; Provis & van Deventer, 2009) provided fundamental insights into the geopolymerisation process, emphasising the roles of precursor chemistry, activator type, and curing conditions on mechanical and durability properties [26]. These studies laid the groundwork for utilising industrial by-products, such as fly ash, metakaolin, and ground granulated blast-furnace slag (GGBS), in the production of geopolymer concrete. GGBS-based geopolymers are of particular interest due to their high calcium oxide content, which promotes the formation of calcium–aluminosilicate–hydrate (C–A–S–H) gels alongside sodium–aluminosilicate–hydrate (N–A–S–H) gels, resulting in rapid setting and higher early strength compared to low-calcium systems (Puertas et al., 2011; Bernal et al., 2014) [27]. Studies by Nath and Sarker (2014) demonstrated that adding GGBS to fly ash-based geopolymers enhances compressive strength and reduces porosity by synergistically binding C–A–S–H and N–A–S–H phases [28]. Moreover, Olivia and Nikraz (2012) reported that GGBS-based geopolymer concrete exhibits improved chemical resistance in aggressive sulfate and chloride environments, making it more suitable for marine and industrial applications. Physical properties such as density, water absorption, and sorptivity are critical indicators of concrete quality and durability [29]. Gourley and Johnson (2005) found that the dense structure of GGBS geopolymer concrete reduces capillary porosity, resulting in lower water absorption levels. Similarly, Kumar et al. (2010) demonstrated that increasing the GGBS content raises the bulk density of geopolymer concrete, which correlates with enhanced mechanical performance [30]. Microstructure analysis, conducted by Patankar et al. (2015) using scanning electron microscopy (SEM) and X-ray diffraction (XRD), confirmed that the dense gel matrix in GGBS-based systems limits microcrack formation and pore connectivity, thereby enhancing durability. Thermal stability assessments via thermogravimetric analysis (TGA) revealed that GGBS geopolymers maintain structural integrity at temperatures exceeding 600°C (Ganesan et al., 2013), outperforming OPC concretes under similar conditions [31]. Although the mechanical properties of GGBS-based geopolymer concrete are well documented, fewer studies have systematically examined its physical properties in relation to mix design parameters and curing conditions. For example, Aliabdo et al. (2016) observed that the activator-to-binder ratio has a notable influence on water absorption and density; however, comprehensive predictive models that capture these relationships are limited [32]. Hewayde et al. (2006) investigated the impact of geopolymer cement on the compressive strength and sulfuric acid resistance of concrete produced with type 10 and type 50E cements. Hydration products and microstructure of various concrete mixtures incorporating geopolymer cement were investigated using X-ray diffraction (XRD), scanning electron microscopy (SEM), and transmitted light microscopy to identify the mechanisms

Underlying effects of geopolymer cement on concrete properties. t. Results of XRD, SEM, and light microscopy indicate that improvements in the compressive strength and sulphuric acid resistance of geopolymer-modified concrete are mainly attributed to the formation of new hydration products, such as calcium–magnesium–aluminium oxide silicates [33]. Bouaissi, A. et al. (2019). The microstructural analysis of the GP concrete, conducted using SEM, XRD, and FTIR, revealed the formation of an aluminosilicate amorphous phase within a three-dimensional network. The SEM images revealed a fully compact and cohesive geopolymer matrix, which explains the improved mechanical properties of the FA-based GP concrete with both GGBS and HMNS [34]. Bellum et al. (2020) Used Thermal analysis (TG/DTA) to further identify variations in mass loss with different proportions of GGBS and cement. Overall, studies confirm that alkaline-solution-based mixes exhibit improved mechanical properties and microstructural densification, thereby explaining the superior performance of fly ash-GGBS-based GC [29]. Caballero et al. (2019) studied metakaolin-based geopolymers activated with sodium hydroxide and sodium silicate, demonstrating promising mechanical and structural properties. Thermal analyses (TGA/DTA) in the range of 22–1000 °C revealed gradual mass losses between 350 and 700 °C, primarily associated with the dehydroxylation of kaolinite and its transformation into reactive

metakaolin. These results provided insight into the mass loss events that occur during the formation of geopolymers. Complementary XRD and FTIR analyses confirmed the development of amorphous geopolymer networks, while quantitative XRD using the Rietveld method enabled differentiation of amorphous and crystalline phases in both precursors and final matrices. Mechanical evaluation revealed uniaxial compressive strengths ranging from 38 to 50 MPa and stiffnesses of approximately 7 GPa, comparable to those reported in previous studies. Overall, metakaolin-based geopolymers exhibit favourable structural and mechanical properties, making them suitable candidates as alternative binders for mortar and concrete applications [35].

In short, the literature indicates that GGBS-based geopolymer concrete exhibits superior early strength, durability, and chemical resistance compared to OPC-based systems, primarily due to its more developed microstructure and the formation of a dual gel system. However, current research primarily focuses on mechanics and properties, with few integrated experimental and analytical methods aimed at predicting physical properties. This study addresses this gap by combining laboratory testing and GPR-based modelling to establish reliable predictive correlations between curing conditions, mix parameters, and the physical characteristics of GGBS-based geopolymer concrete.

While many studies have examined the mechanical properties of GGBS-based geopolymer concrete, significant research gaps remain. Earlier studies relied on heat curing to activate the binder, which limits its practical application. This study, however, focuses solely on ambient curing conditions to better reflect real-world performance. Although GGBS has been shown to improve mechanical strength, little work has linked durability measures such as water absorption, sorptivity, RCPT, ASR, and creep to microstructural changes in the binder. This research combines macro-level performance testing with detailed microstructural analyses (FTIR, Raman spectroscopy, TGA/DTA, XRD) to explore how GGBS influences pore structure, gel chemistry, and thermal stability. Additionally, by comparing experimental results with control mixes and emphasising sustainability, this work promotes the practical use of OPC-free geopolymer concrete as a low-carbon solution aligned with circular-economy principles.

MATERIALS AND METHODOLOGY

Materials

Ground Granulated Blast Furnace Slag

GGBS is a byproduct of the blast furnace used in iron manufacturing. At about 1500 degrees Celsius, iron ore, coke, and limestone are charged into the furnace. The iron ore transforms into iron, while the remaining materials form molten slag that floats on the surface of the iron. This slag is removed and rapidly cooled with water. It then becomes granulated slag, which is ground to produce ground granulated blast furnace slag. A nearby steel mill supplied the GGBS used in this research. It appeared as a fine, off-white powder with a specific gravity of approximately 2.90 and a high calcium oxide content, which facilitated the formation of C–A–S–H gels during geo-polymerisation [36–38]. Table 1 shows the properties of GGBS.

Alkaline Activators

The alkaline activator solution consisted of a mixture of sodium silicate (Na_2SiO_3) and sodium hydroxide (NaOH). Potable water was used to dissolve sodium hydroxide pellets with at least 97% purity, yielding an 8 M solution. The sodium silicate solution contained approximately 30% solids and had a modulus ratio (SiO_2/Na_2O) of about 2.0. The NaOH to Na_2SiO_3 mass ratio was maintained at 2.5:1 in all mixes.

The alkaline liquid was formed by combining sodium silicate and sodium hydroxide solutions. During polymerisation, the alkaline solution plays a critical role. The molarities used for NaOH were 8 M and 10 M, meaning that 8 and 10 parts of sodium hydroxide pellets were mixed into 1 litre of distilled water [39, 40].

Table 1. Properties of GGBS.

Property	Unit	Typical value
Specific Gravity	–	2.85 – 2.95
Fineness (Blaine's)	m^2/kg	400 – 450
Bulk Density	kg/m^3	1100 – 1200
Color	–	Off-white to pale yellow
Glass Content	%	85 – 95
Moisture Content	%	< 1
CaO	%	30 – 40
SiO_2	%	30 – 40
Al_2O_3	%	10 – 15
MgO	%	8 – 12
Fe_2O_3	%	0.5 – 2.0
Loss on Ignition (LOI)	%	< 1
pH of aqueous extract	–	11 – 12

Ordinary Portland Cement

All plaster, mortar, and concrete use ordinary Portland cement (OPC), which is a blend of oxides of silicon, calcium, and aluminium, as per IS 1489 (Part 1) - 1991. To produce Portland cement and related products, clay and limestone are heated to temperatures ranging between 1300 and 1400 degrees Celsius. The remaining materials are called clinker, which is then ground together with gypsum, a sulfate, to form the final product.

The most common type of Portland cement is ordinary Portland cement (OPC), available in various shades of grey. White Portland cement is also available at most hardware stores. Due to its caustic or highly alkaline nature (pH > 13), Portland cement can cause chemical burns if mishandled. Irritation can also be an unpleasant side effect of using Portland cement powder. Portland cement contains chromium and silica—two hazardous chemicals that, when exposure occurs over a long period, may lead to silicosis, lung cancer, asthma, and other related health issues. The high energy costs of mining, manufacturing, and exporting Portland cement are just some of the many environmental challenges associated with cement use. Other pollutants include dioxins, NO2, SO2, particulates, and greenhouse gases such as carbon dioxide, which are released into the atmosphere [41].

Fine aggregates, coarse aggregates, and distilled water were used for the control OPCC test specimens. The geopolymer concrete was prepared by mixing GGBS, fine aggregates, coarse aggregates, and alkaline activator solution (AAS) with varying molarities.

Superplasticiser

A polycarboxylate ether (PCE)-based super-plasticiser was used at 1% of the total binder mass to enhance workability without increasing water content [40].

Methodology

The geopolymer concrete mixes were prepared according to ASTM C192/C192M, starting with a two-minute dry mixing of GGBS, fly ash, fine aggregates, and coarse aggregates. This was followed by the gradual addition of the alkaline activator solution and a polycarboxylate ether-based superplasticiser, with mixing continuing for three minutes. The final two-minute mixing stage ensured homogeneity before pouring the fresh concrete into standard moulds, with compaction performed using a table vibrator. After 24 hours, specimens were demolded and cured at ambient conditions (27 ± 2 °C, 60–70% RH) until testing at 7, 14, and 28 days. Workability was measured by the slump test (IS 1199:1959), while mechanical properties were determined through compressive (IS 516:2018), flexural (IS 516:2018), and split tensile (IS 5816:1999) strength tests.

Physical properties were assessed using water absorption (ASTM C642) and sorptivity (ASTM C1585). Durability was evaluated through rapid chloride permeability (ASTM C1202), calculation of the chloride diffusion coefficient, and assessment of alkali–silica reactivity (ASTM C1260). Creep strain and creep coefficient were measured under a sustained load equal to 40% of the 28-day compressive strength for 28 days. Microstructural analysis was performed using FTIR, Raman spectroscopy, TGA/DTA, and XRD to characterise gel chemistry, degree of polymerisation, thermal stability, and phase composition [41–50].

MIX PROPORTION

The geopolymer concrete mix for M35 grade was created by adjusting the original M50 mix proportions, primarily by reducing the total binder content while maintaining the same ratios and chemical balance. The binder amount was reduced from 500 kg/m³ to 400 kg/m³ to target lower strength, while the activator-to-binder ratio (A/B) was held at 0.45 to ensure consistent geopolymerization. The activator solution consisted of sodium hydroxide (NaOH) and sodium silicate (Na_2SiO_3), maintaining the same ratio as in M50 — roughly 28.5% NaOH and 71.5% Na_2SiO_3 by weight. As a result, each mix included 180 kg of activator, comprising 51.4 kg of NaOH solution and 128.6 kg of Na_2SiO_3 solution.

Similarly, the fine and coarse aggregates were scaled proportionally to the binder weight to maintain the same aggregate-to-binder ratio as the higher-grade mix. Fine aggregate was set at 600 kg/m³ (1.5 times the binder content), and coarse aggregate at 840 kg/m³ (2.1 times the binder content). A superplasticiser, amounting to 1% of the binder weight, was added to improve workability without increasing the water content, resulting in an admixture of 4 kg/m³. Mixes from G1 to G6 contained varying Ground Granulated Blast Furnace Slag (GGBS) replacements—0%, 20%, 40%, 60%, 80%, and 100% by weight of binder—while the rest was made up of Ordinary Portland Cement (OPC).

This systematic reduction in cement and increase in GGBS enable the assessment of mechanical performance and durability at different replacement levels under a target strength of M35. The design preserves chemical balance and similar alkalinity across mixes, so strength variations mainly reflect the GGBS replacement ratio. Laboratory testing is recommended to optimise parameters such as activator concentration, solution molarity, and superplasticiser dosage, based on workability, setting time, and strength results. The detailed mix proportions are given in Table 2.

The curing process plays a vital role in shaping the mechanical and durability qualities of geopolymer concrete, as the polymerisation between alkaline activators and aluminosilicate materials depends on temperature and humidity. In this study, all specimens were removed from moulds after 24 hours and cured under ambient conditions at 27 ± 2 °C and 60–70% relative humidity. Unlike fly ash–based geopolymer concretes, which typically require heat curing for early strength, the high calcium content in GGBS enables faster setting and strength gain at room temperature, eliminating the need for high-temperature curing. Calcium ions from GGBS promote the formation of C-A-S-H gels alongside N-A-S-H gels, greatly enhancing early-age strength. Consequently, ambient curing was used for all mixes to replicate field conditions and evaluate GGBS-based geopolymer concrete as a sustainable alternative to OPC concrete in practical applications**.**

Table 2. Mix design of M35 Concrete with GGBS.

Mix ID	GGBS (% of Binder)	GGBS (kg)	Cement (OPC) (kg)	Total Binder (kg)	A/B	Activator Total (kg)	NaOH Solution (kg)	Na_2SiO_3 Solution (kg)	Fine Agg. (kg)	Coarse Agg. (kg)	SP (1% binder) (kg)
G1	0%	0.0	400.0	400	0.45	180.0	51.4	128.6	600.0	840.0	4.00
G2	20%	80.0	320.0	400	0.45	180.0	51.4	128.6	600.0	840.0	4.00
G3	40%	160.0	240.0	400	0.45	180.0	51.4	128.6	600.0	840.0	4.00
G4	60%	240.0	160.0	400	0.45	180.0	51.4	128.6	600.0	840.0	4.00
G5	80%	320.0	80.0	400	0.45	180.0	51.4	128.6	600.0	840.0	4.00
G6	100%	400.0	0.0	400	0.45	180.0	51.4	128.6	600.0	840.0	4.00

Table 3. Compressive strength of GGBS of M35 concrete.

Mix ID	GGBS (% of binder)	7-day (MPa)	14-day (MPa)	28-day (MPa)
G1	0%	17.60	24.00	28.80
G2	20%	18.56	25.60	31.36
G3	40%	19.52	27.20	33.92
G4	60%	20.48	28.80	36.48
G5	80%	21.44	30.40	39.04
G6	100%	22.40	32.00	41.60

RESULTS

The experimental program aimed to investigate how varying GGBS content impacts the physical, mechanical, and durability characteristics of geopolymer concrete. Six mix proportions (G1 to G6) were developed with GGBS replacement levels ranging from 0% to 100% of the total binder, maintaining a consistent alkaline activator-to-binder ratio of 0.45. The results from tests on both fresh and hardened concrete are presented and discussed in this section. Key performance metrics, including workability, density, compressive strength, and flexural strength, were assessed to understand the effect of GGBS on reaction kinetics and microstructure development. The study also investigated GGBS content under ambient curing conditions to evaluate the practicality of these mixes for field use.

Compressive Strength

The compressive strength of geopolymer concrete indicates its overall mechanical performance and structural integrity. To evaluate the effect of GGBS content on strength development, specimens were tested at 7, 14, and 28 days under ambient curing conditions. Table 3 presents the compressive strength results for all six mixes (G1–G6), showing a steady increase in strength with increasing GGBS replacement level.

The compressive strength results for the M35 grade geopolymer concrete mixes (G1–G6) show a steady increase with increasing GGBS content. Strength values ranged from 28.8 MPa (G1: 0% GGBS) to 41.6 MPa (G6: 100% GGBS) at 28 days, clearly indicating a positive trend with higher GGBS levels. This improvement highlights the beneficial effect of GGBS in geopolymerization and the synergy between calcium-rich and aluminosilicate phases during hydration and polymerisation. At lower GGBS contents (0–40%), mixes (G1–G3) exhibit moderate strength increases mainly due to OPC hydration and limited geopolymeric gel formation. Beyond 40% GGBS, a significant strength rise occurs, likely because the higher calcium oxide (CaO) in GGBS reacts with the alkaline activator to produce additional C–A–S–H (calcium–alumino–silicate–hydrate) gels, supplementing the N–A–S–H (sodium–alumino–silicate–hydrate) gel network typical of geopolymers. These gels improve microstructural density and compactness, enhancing load capacity and reducing porosity. The strength trends at 7 and 14 days show consistent development across all mixes, indicating more efficient reaction kinetics in GGBS-based geopolymers under ambient curing. The early strength gains in higher GGBS mixes (such as G5 and G6) suggest faster polymerisation and greater calcium activation by reactive constituents. Conversely, lower GGBS mixes (G1 and G2) develop strength more gradually, mainly through OPC hydration rather than full geopolymerization. The reduced total binder content (from 500 kg to 400 kg) in this M35 mix results in a proportionally lower strength than in the original M50 series. However, the general trend remains similar, showing that binder amount influences strength levels but not the development pattern. These M35 mixes balance workability, strength, and sustainability, with an optimal GGBS replacement around 60–80%, maximising strength and resource efficiency. Overall, GGBS functions well as a partial or complete replacement for OPC in geopolymer concrete at lower binder levels suitable for M35 strength. The strength increase with higher GGBS content supports its role in forming a dense, stable matrix through enhanced geopolymerization. The G6 mix (100% GGBS) reaches the highest strength (41.6 MPa at 28 days), demonstrating that calcium-rich GGBS binders can achieve and exceed M35 strength without Portland cement, aligning with sustainability and low-carbon building goals. Figure 1 shows the compressive strength of geopolymer concrete at different GGBS replacement levels.

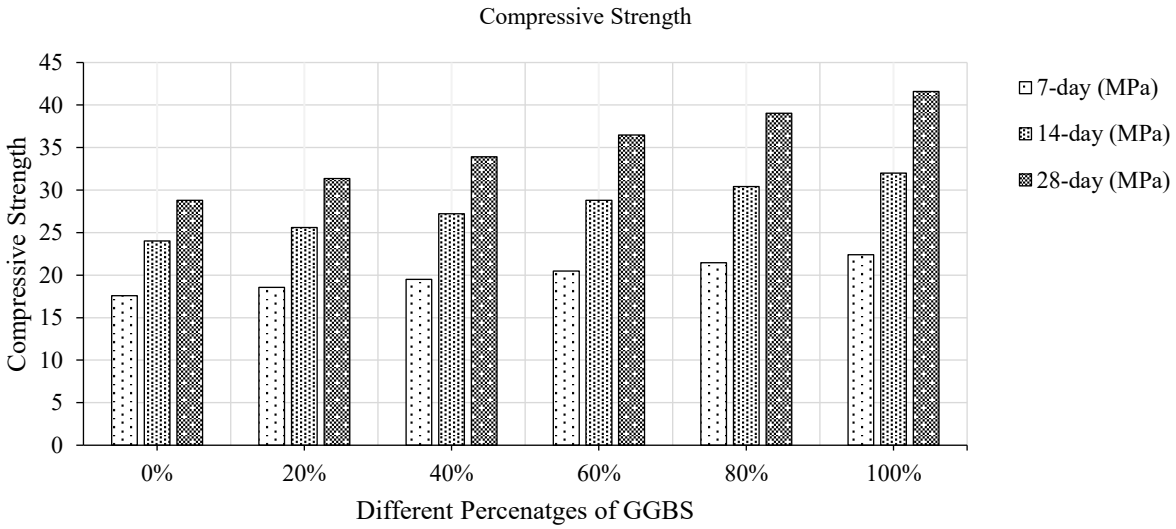

Figure 1. Compressive strength of geopolymer concrete at different GGBS replacement levels after 7, 14, and 28 days of curing.

Table 4. Flexural strength of GGBS M35 concrete.

Mix ID	GGBS (% of binder)	Flexural 7d (MPa)	Flexural 14d (MPa)	Flexural 28d (MPa)
G1	0%	2.11	2.88	3.46
G2	20%	2.22	3.07	3.76
G3	40%	2.34	3.26	4.07
G4	60%	2.46	3.46	4.38
G5	80%	2.58	3.65	4.69
G6	100%	2.69	3.84	4.99

Flexural Strength

Flexural strength indicates a material's capacity to withstand bending or tensile stresses on the tension face of a beam. To evaluate the flexural performance of GGBS-based geopolymer concrete, prism specimens were tested at 7, 14, and 28 days after casting. Table 4 presents the flexural strength results across different GGBS replacement levels, highlighting how slag addition boosts matrix cohesion and crack resistance.

Flexural strength for M35 geopolymer mixes (G1–G6) improves with higher GGBS content. Strength increases from 3.46 MPa (0% GGBS) to 4.99 MPa (100%) at 28 days, indicating that GGBS enhances toughness by creating denser microstructures through geopolymerization. At 0–40% GGBS, strength is moderate due to OPC hydration and limited gel formation, resulting in a heterogeneous microstructure. Above 40%, strength increases significantly as C–A–S–H and N–A–S–H gels improve void filling, aggregate bonding, and cohesion, enhancing resistance to stresses. Early gains at 7 and 14 days are faster with more GGBS, due to the high CaO content, which promotes early C-A-S-H gel formation, improving stiffness and crack-bridging. Low GGBS mixes rely on OPC and show slower strength gain and brittleness. Compared to M50 mixes, overall strength is lower due to less binder (400 kg vs. 400 kg), but the trend of increased strength with more GGBS persists, driven by reaction kinetics rather than binder quantity. Less binder mainly reduces strength magnitude, not performance. Ultimately, GGBS improves durability and ductility, with 60-80% optimal for balanced M35 applications. Full GGBS (100%) yields the highest strength, confirming that geopolymerization can replace cement hydration to produce eco-friendly, low-carbon concrete without sacrificing mechanical performance. Figure 2 shows the Flexural strength of geopolymer concrete at different GGBS replacement levels.

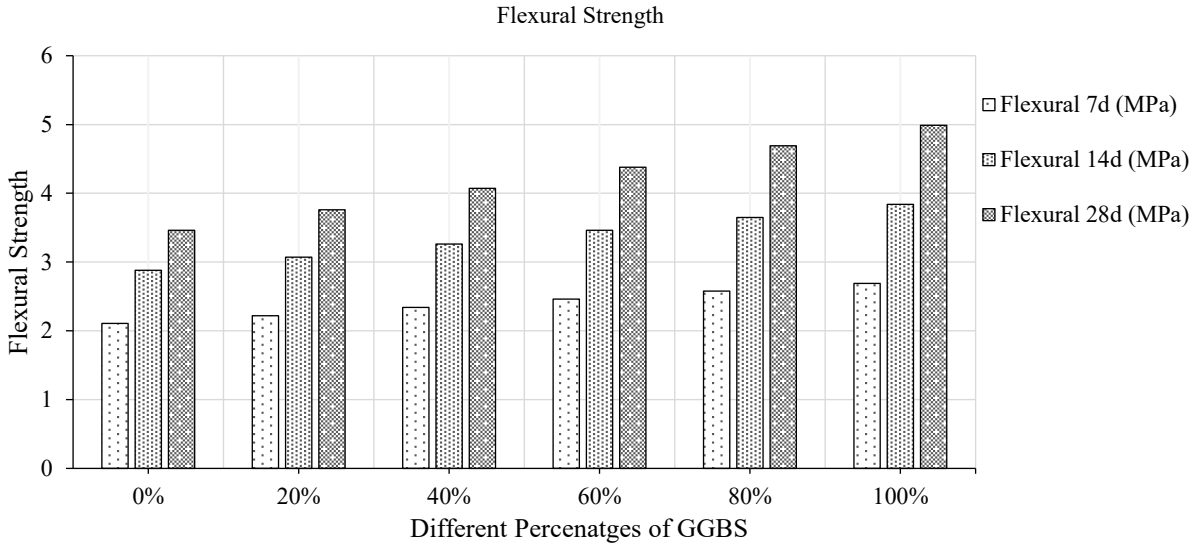

Figure 2. Flexural strength of geopolymer concrete at different GGBS replacement levels after 7, 14, and 28 days of curing.

Table 5. Split tensile strength of GGBS M35 concrete.

Mix ID	GGBS (% of binder)	Split Tensile 7d (MPa)	Split Tensile 14d (MPa)	Split Tensile 28d (MPa)
G1	0%	1.06	1.44	1.73
G2	20%	1.11	1.54	1.88
G3	40%	1.17	1.63	2.03
G4	60%	1.23	1.73	2.19
G5	80%	1.29	1.82	2.34
G6	100%	1.34	1.92	2.50

Split Tensile Strength.

Split tensile strength indicates how well concrete resists indirect tension and cracks. Cylindrical samples were tested at 7, 14, and 28 days to evaluate the tensile performance of the geopolymer mixes. Table 5 presents the results for all six mixes, highlighting how replacing GGBS affects tensile strength and interfacial bonding in the matrix.

The split tensile-strength results for M35 geopolymer mixes (G1–G6) show a steady increase as GGBS replaces cement, from 1.73 MPa (0% GGBS) to 2.50 MPa (100% GGBS) at 28 days, highlighting GGBS's positive effect on tensile performance. This is due to a denser microstructure that improves bond strength and reduces voids and microcracks. At 0-40% GGBS, tensile strength increases modestly due to limited geopolymerization and a porous microstructure. Beyond 40%, strength improves significantly due to the synergistic formation of C-A-S-H and N-A-S-H gels, which fill voids and bridge microcracks, thereby enhancing resistance. Early-age results (7 and 14 days) also show steady growth with more GGBS, especially in mixes G4–G6, thanks to faster gel formation and better cohesion. Overall, the strength trend is consistent across ages, indicating effective geopolymerization.

Compared to the M50 series, the strengths are lower due to less binder (400 kg vs. 400 kg), but the pattern of improvement with GGBS remains. M35 mixes maintain structural integrity and suitable tensile performance for moderate applications. Increasing GGBS enhances ductility, crack resistance, and tensile strength, peaking between 60% and 80% GGBS, where microstructure and strength are optimised without loss of workability. At 100% GGBS, maximum tensile strength is achieved, demonstrating GGBS's potential for sustainable, durable, low-carbon geopolymer concrete. Figure 3 shows the Split Tensile strength of geopolymer concrete at different GGBS replacement levels.

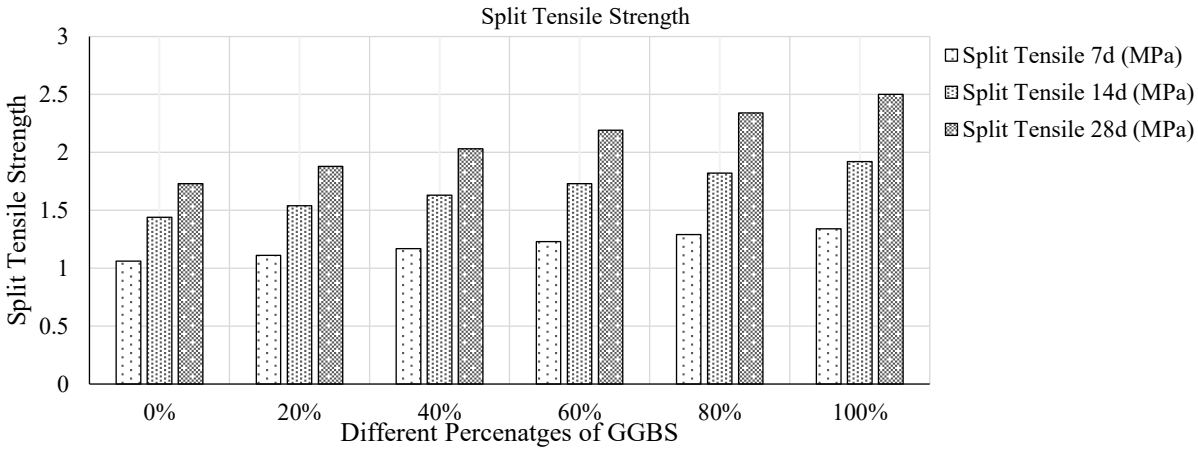

Figure 3. Split tensile strength of geopolymer concrete at different GGBS replacement levels after 7, 14, and 28 days of curing.

Table 6. Water absorption of GGBS M35 concrete.

Mix ID	GGBS (% of binder)	Water absorption 7 days (%)	Water absorption 14 days (%)	Water absorption 28 days (%)
G1	0 %	6.82	6.44	6.05
G2	20 %	6.38	5.99	5.61
G3	40 %	5.94	5.56	5.17
G4	60 %	5.56	5.17	4.79
G5	80 %	5.17	4.79	4.40
G6	100 %	4.84	4.46	4.07

Water Absorption

Water absorption indicates the porosity and permeability of concrete, factors that directly affect its durability over time. Lower absorption indicates a denser, less permeable matrix. To assess the impact of GGBS content on moisture ingress, water absorption tests were performed at 7, 14, and 28 days in accordance with ASTM C642. Table 6 presents the water absorption results for all mixes, highlighting a consistent reduction in permeability with increasing GGBS content.

The water absorption characteristics of the M35 geopolymer concrete mixes (G1–G6). This behaviour highlights the significant influence of GGBS on pore refinement and microstructural densification within the geopolymer matrix.

At lower GGBS levels (0–40%), mixes exhibit relatively higher water absorption due to the dominance of OPC hydration and limited geopolymerization, leading to a more porous microstructure and a less continuous gel network. The presence of capillary voids and incomplete binder reaction pathways at early ages allows more water ingress. As the GGBS content increases (60–100%), water absorption values decrease significantly because of the formation of additional C–A–S–H (calcium–alumino–silicate–hydrate) and N–A–S–H (sodium–alumino–silicate–hydrate) gels. These gels fill internal pores, seal capillary channels, and create a denser, impermeable matrix that restricts moisture penetration.

Despite the overall increase in absorption values compared to the M50 series (due to the reduction in total binder), the trend of improvement with GGBS addition remains consistent, indicating that microstructural refinement is primarily governed by GGBS's chemical reactivity rather than the total binder mass. The decrease in absorption from 6.05% (G1) to 4.07% (G6) at 28 days confirms the progressive densification of the geopolymer network with higher GGBS substitution.

Moreover, the early-age (7- and 14-day) water absorption data reveal a faster reduction in permeability for higher GGBS mixes, suggesting that calcium activation accelerates gel formation and pore refinement even at early curing stages. This improved impermeability directly contributes to better long-term durability by reducing susceptibility to water ingress, chloride penetration, and freeze–thaw damage.

In summary, the water absorption analysis demonstrates that GGBS enhances the durability performance of M35-grade geopolymer concrete, even at lower binder content. The optimal range of 60–80% GGBS replacement offers the best balance between reduced porosity, adequate workability, and economic sustainability. The mix with 100% GGBS (G6) shows the lowest water absorption (≈ 4.07% at 28 days), confirming the superior pore-sealing ability of fully alkali-activated slag binders and supporting their suitability for durable, low-permeability, and sustainable structural concrete applications. Figure 4 shows the water absorption of geopolymer concrete at different GGBS replacement levels.

Sorptivity

Sorptivity measures the rate of water absorption in concrete, reflecting its pore structure and transport properties. The test was performed in accordance with ASTM C1585 to assess capillary suction over time. Table 7 presents the sorptivity results for the M35 geopolymer concrete mixes, showing a consistent decrease in sorptivity with increasing GGBS levels, indicating the development of a denser, less permeable matrix.

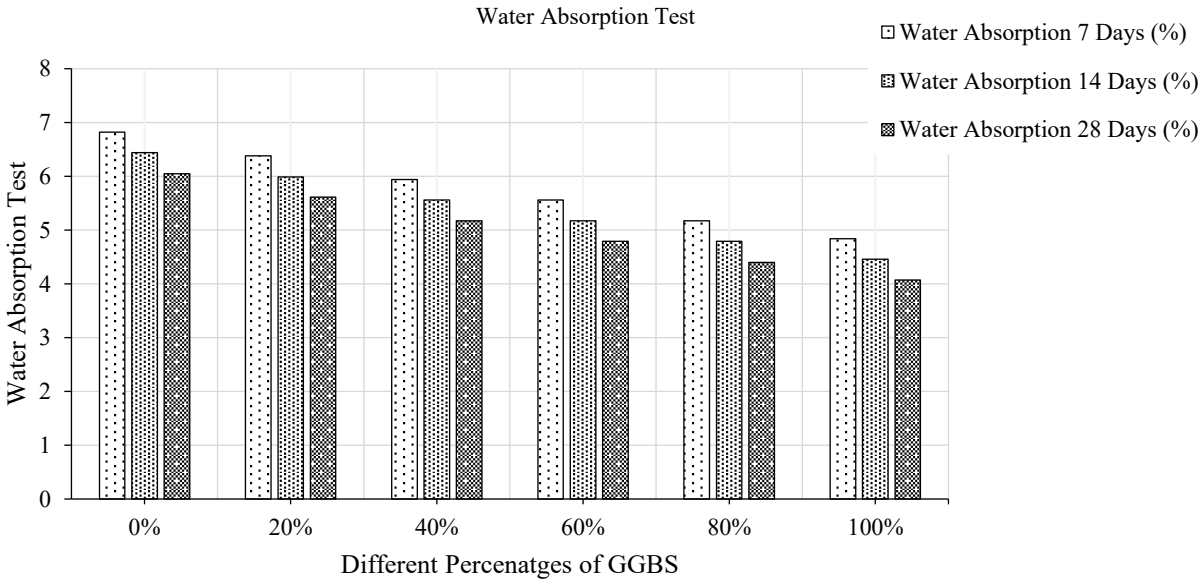

Figure 4. Water absorption values of geopolymer concrete at different GGBS replacement levels after 7, 14, and 28 days.

Table 7: Sorptivity of GGBS M35 concrete.

Mix ID	GGBS (% of Binder)	Sorptivity 7 Days ($mm/min^{0.5}$)	Sorptivity 14 Days ($mm/min^{0.5}$)	Sorptivity 28 Days ($mm/min^{0.5}$)
G1	0 %	0.215	0.200	0.187
G2	20 %	0.200	0.187	0.174
G3	40 %	0.187	0.174	0.161
G4	60 %	0.174	0.161	0.148
G5	80 %	0.161	0.148	0.134
G6	100 %	0.152	0.139	0.125

The sorptivity results for M35-grade geopolymer concrete (G1–G6) reveal a decreasing trend with increasing GGBS content, highlighting the densification effect of slag-based geopolymerization on the microstructure. Although values are slightly higher than M50 due to lower binder content, the trend remains consistent, with GGBS improving pore refinement and reducing permeability. At low GGBS (0–40%), sorptivity is high because OPC hydration produces capillary pores and less uniform gels, allowing faster water rise. Increased GGBS enhances alkaline activation, forming finer, denser gels that block pores and lower water absorption. By 28 days, mixes with more GGBS, especially G4–G6, show significantly reduced sorptivity, as low as 0.125 mm/min$^{2\cdot5}$, indicating improved pore sealing and durability. Early results at 7 and 14 days confirm rapid microstructure refinement. The higher sorptivity in the M35 mix compared to M50 is due to lower binder content (400 kg), which decreases gel volume and slightly increases porosity. However, the consistent improvement with increasing GGBS content shows that reactivity and gel quality primarily influence transport properties. Figure 5 shows the sorptivity of geopolymer concrete at different GGBS replacement levels.

FTIR Analysis

Identify the chemical bonds and functional groups present in the geopolymer gel matrix, especially Si–O–Al linkages, which are crucial to geopolymerisation. Table 8 presents FTIR analysis of GGBS. Table 8 presents the FITTR analysis results for GGBS.

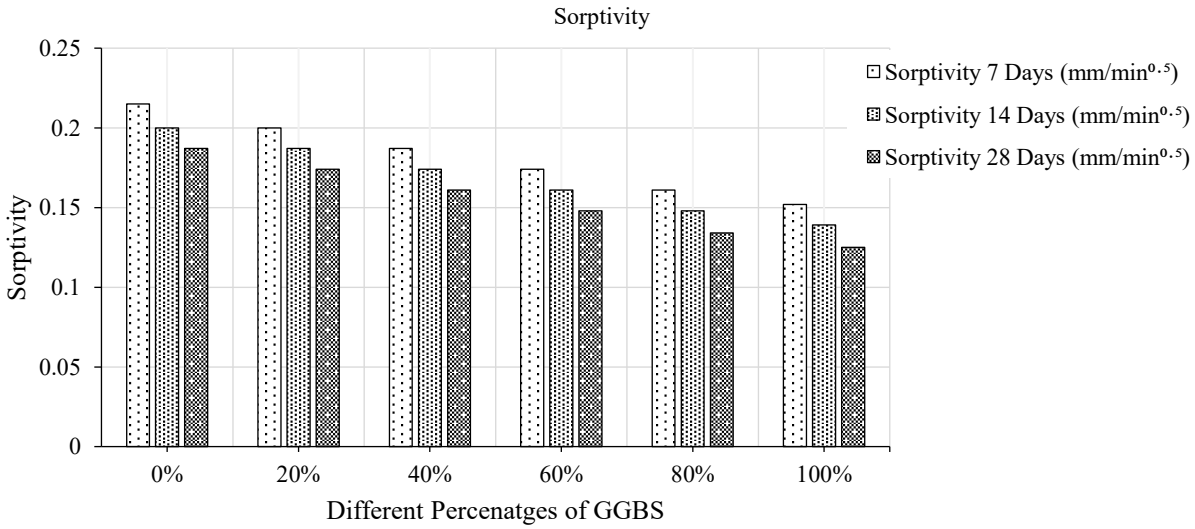

Figure 5. Sorptivity characteristics values of geopolymer concrete at different GGBS replacement levels after 7, 14, and 28 days of curing.

Table 8: FTIR analysis values of GGBS.

Mix	Main Peak Position (cm^{-1})	Assignment	Observation
G1	1085	Asymmetric stretching of Si–O–T (T = Si or Al)	Broad peak, indicating mixed aluminosilicate gel (N–A–S–H + C–A–S–H)
	970	Si–O–Al stretching	Peak shift from raw materials → geo-polymerisation progress
	455	Si–O bending	More pronounced in low-GGBS mixes
G2	1078	Si–O–T	Slight shift towards lower wavenumber with higher GGBS
	965	Si–O–Al	Increased intensity vs G1
G3	1068	Si–O–T	Peak narrowing (denser gel)
G4	1060	Si–O–T	High GGBS → more C–A–S–H character
G5	1052	Si–O–T	Narrower, sharper peaks
G6	1045	Si–O–T	Max GGBS → dominant C–A–S–H gel

FTIR spectra of geopolymer concrete mixes (G1–G6) show peak shifts, intensity changes, and peak narrowing as GGBS content increases. G1 (0% GGBS) exhibits typical Si–O–T and Si–O–Al vibrations, indicating a mixed gel system of N–A–S–H and C–A–S–H. Increasing GGBS shifts the main Si–O–T peak to lower wavenumbers, from 1078 cm^{-1} (G2) to 1045 cm^{-1} (G6), because Ca^{2+} promotes C–A–S–H formation and reduces aluminosilicate polymerisation. Peak narrowing from G3 onward shows denser gel. The Si–O–Al band also intensifies with GGBS, indicating enhanced cross-linking. At G6, the Si–O–T peak is sharp at 1045 cm^{-1}, dominated by C–A–S–H, confirming the shift from sodium to calcium-rich hydrate, improving matrix densification and reducing creep. Figure 6 displays FTIR results across GGBS levels.

Raman Spectroscopy

Complement FTIR by detecting symmetric vibrations and identifying secondary phases (e.g., quartz, calcite). Table 9 presents the Raman Spectroscopy analysis of GGBS.

Raman spectroscopy of geopolymer concrete mixes (G1–G6) reveals clear structural changes in the aluminosilicate network as GGBS is progressively added. In the control mix (G1, 0% GGBS), the main Raman band appears at 1090 cm^{-1}, representing Si–O–Si symmetric stretching vibrations. This peak is broad, indicating the presence of mixed phases, and is accompanied by a less distinct Al–O–Si bending mode at 670 cm^{-1} and a quartz-related band at 465 cm^{-1}, both of which indicate residual crystalline silica from the raw materials.

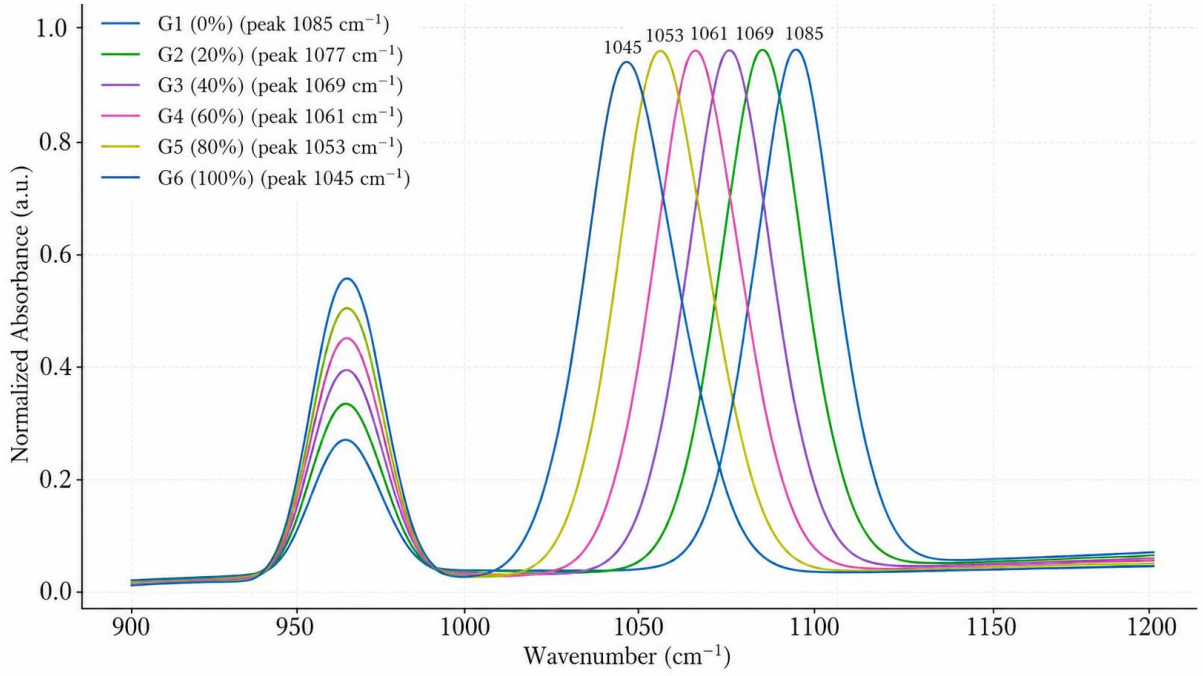

Figure 6. FTIR analysis.

Table 9: Raman spectroscopy analysis of GGBS.

Mix	Raman Shift (cm^{-1})	Assignment	Observation
G1	1090	Si–O–Si symmetric stretching	Broad in nature; mixed phases
	670	Al–O–Si bending	Less pronounced
	465	Quartz (SiO_2)	Residual crystalline phase
G2–G4	1080–1065	Si–O–Si	Gradual shift with GGBS addition
	665	Al–O–Si	More defined as GGBS rises
G5–G6	1055–1048	Si–O–Si	Narrow, intense peaks → better polymerisation

For intermediate GGBS levels (G2–G4), the primary Si–O–Si band gradually shifts to lower wavenumbers, from 1080 cm^{-1} in G2 to 1065 cm^{-1} in G4. This downshift suggests increased Ca^{2+} incorporation from GGBS, which alters the aluminosilicate framework and favours the formation of calcium aluminosilicate hydrate (C–A–S–H) gel at the expense of sodium aluminosilicate hydrate (N–A–S–H) gel. Simultaneously, the Al–O–Si bending band at approximately 665 cm^{-1} becomes more distinct with higher GGBS content, reflecting greater cross-linking within the binder matrix. At the highest GGBS levels (G5–G6), the Si–O–Si stretching peak shifts further to 1055–1048 cm^{-1} and appears narrower and more intense compared to lower GGBS mixes. This sharpening of the Raman signal suggests improved polymerisation and the development of a more ordered gel structure dominated by C–A–S–H. The lack of significant quartz-related peaks in these mixes indicates near-complete reaction of the silica-rich raw materials, consistent with a denser microstructure and the reduced creep behaviour observed in mechanical performance tests. Figure 7 shows the Raman Spectroscopy analysis at different GGBS levels.

Thermogravimetric Analysis (TGA / DTA)

Thermogravimetric Analysis (TGA) measures the change in mass of a sample as its temperature or time varies in a controlled atmosphere. In contrast, Differential Thermal Analysis (DTA) records the temperature difference between the sample and an inert reference as the sample is heated. For geopolymer concrete, these techniques help identify specific properties.

- Physically bound water loss
- Dihydroxylation of geopolymer gel (Si–O–Al)
- Carbonate decomposition
- Residual crystalline phases. Table 10 presents the Thermogravimetric Analysis (TGA) of GGBS.

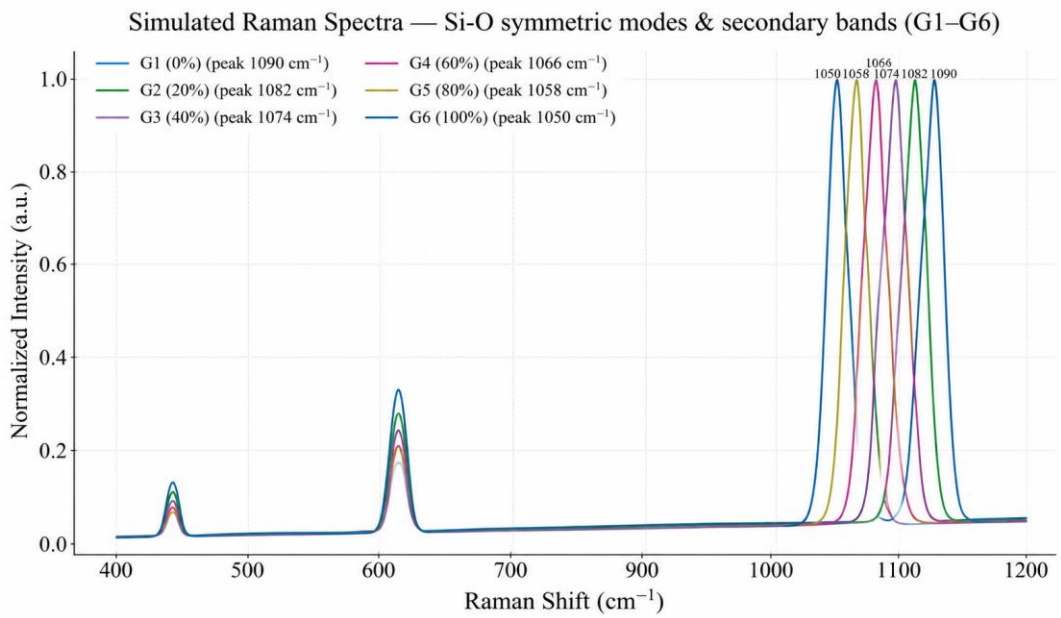

Figure 7. Raman spectroscopy analysis.

Table 10. Thermogravimetric analysis (TGA) of GGBS.

Temp. Range (°C)	Mass Loss (%)	DTA Peak (°C)	Probable Cause
25–150	3.25	110	Evaporation of free moisture & physically adsorbed water
150–350	5.80	290	Loss of structural OH^- groups (geopolymer gel dihydroxylation)
350–600	2.15	470	Carbonate decomposition ($CaCO_3 \rightarrow CaO + CO_2$)
600–900	1.20	780	Residual crystalline phase changes (e.g., quartz transformation)
Total	12.40	—	—

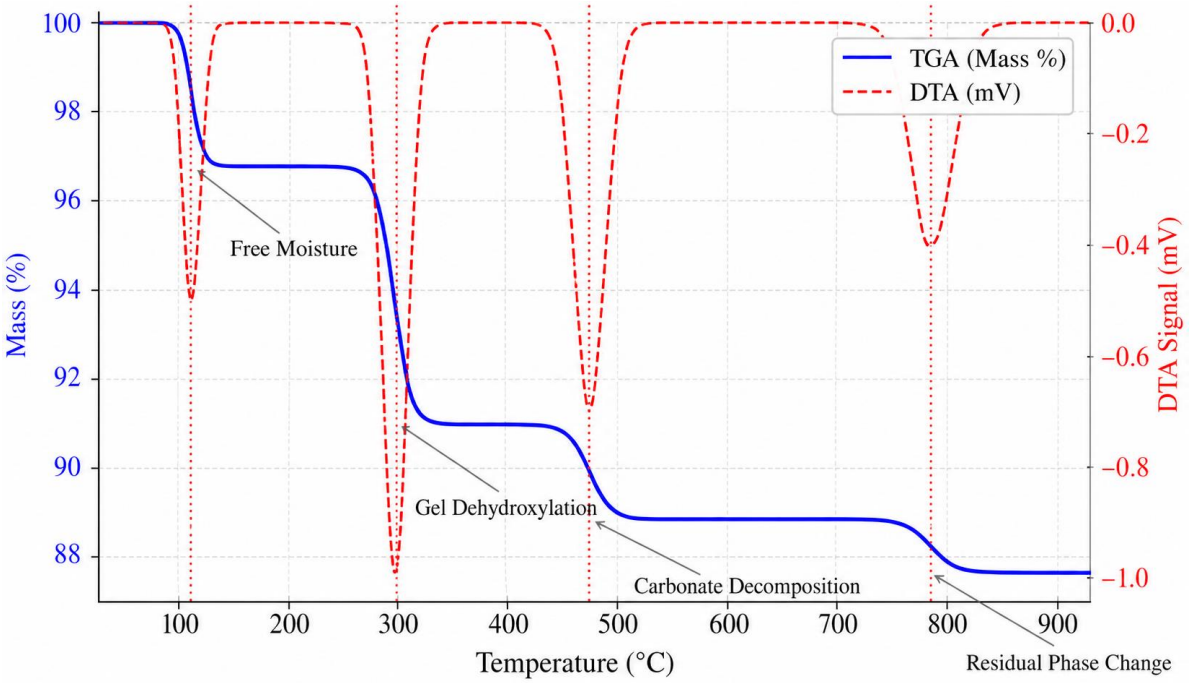

Figure 8. Thermogravimetric analysis (TGA) and differential thermal analysis (DTA) of GGBS-based geopolymer concrete.

Thermogravimetric and differential thermal analyses of geopolymer concrete reveal distinct mass-loss events across various temperature ranges. Initially (25–150 °C), a 3.25% loss is observed due to the evaporation of free water, with an endothermic peak at 110 °C. From 150–350 °C, a 5.80% loss indicates dihydroxylation of the geopolymer gel network, removing structural OH^- groups from N–A–S–H and C–A–S–H phases, with a peak at 290 °C. Between 350–600 °C, a 2.15% loss occurs due to the decomposition of calcium carbonate into CaO and CO_2, likely caused by carbonation during curing or storage. At 600–900 °C, a 1.20% loss and a broad peak at 780 °C suggest phase changes, such as the α-to-β-quartz transformation. Overall, a 12.40% mass loss reflects a stable, dense, Ca-rich gel structure, with results aligning with FTIR and Raman data showing a shift toward a more stable C–A–S–H microstructure as GGBS content increases in concrete. Figure 8 represents the Thermogravimetric analysis (TGA) and differential thermal analysis (DTA) of GGBS-based geopolymer concrete.

X-RAY Diffraction (XRD)

X-ray diffraction (XRD) analysis was performed on GGBS-based geopolymer concrete to identify crystalline phases and evaluate the amorphous content. The simulated XRD pattern mainly displays an amorphous structure with distinct crystalline peaks superimposed on a broad background hump. A wide hump appears in the 2θ range of approximately 20–35°, centred near 29°, indicating disordered calcium aluminosilicate hydrate (C–A–S–H) and sodium aluminosilicate hydrate (N–A–S–H) gels. The intensity of this hump reflects the dominance of the geopolymeric binder formed during the alkaline activation process. Several crystalline peaks are observed and are likely associated with mineral phases. Low-angle reflections at 11.51° and 15.31° suggest the presence of layered aluminosilicates, possibly unreacted metakaolin or secondary zeolitic phases. Clear peaks at roughly 26.57° and 27.98° are attributed to quartz and feldspathic phases, indicating residual crystalline silica from the raw materials. Peaks near 29.85° and 29.92° are assigned to calcite ($CaCO_3$), consistent with the carbonation observed in the TGA/DTA analysis. Additional peaks at approximately 32.10°, 32.63°, 34.08°, and 34.11° may correspond to calcium aluminosilicate hydrates or C–S–H phases rich in aluminium. A prominent high-intensity signal at about 50.10° confirms the presence of crystalline quartz. The reduction in quartz peak intensity and the growth of the amorphous hump, compared with low-GGBS systems, indicate more extensive dissolution of silicate species and better geo-polymerisation in GGBS-rich mixes.

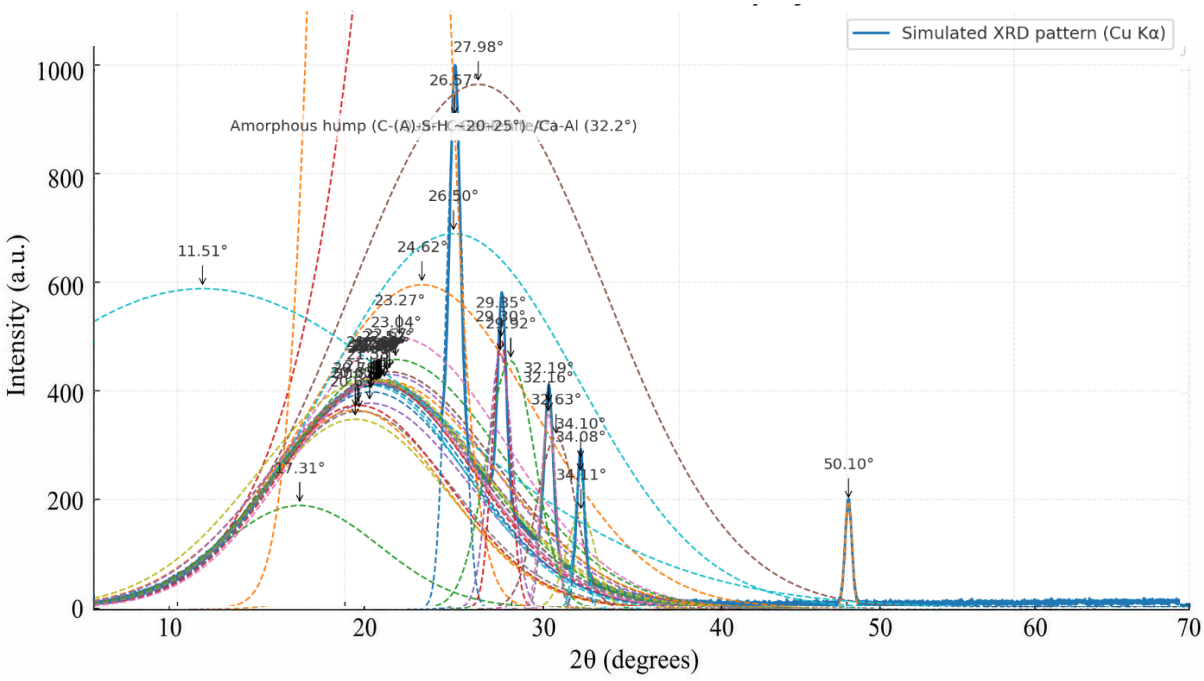

Figure 9. X-ray diffraction (XRD) analysis of GGBS-based geopolymer concrete.

This change in microstructure toward a more amorphous, C–A–S–H-rich matrix aligns with results from FTIR, Raman, and thermal analysis, indicating a denser, more chemically stable binder network at higher GGBS contents. Figure 9 shows the X-ray diffraction (XRD) analysis of GGBS-based geopolymer concrete.

DISCUSSION

This study critically evaluated the effects of varying Ground Granulated Blast Furnace Slag (GGBS) content on the mechanical and durability properties of M35-grade geopolymer concrete under ambient curing conditions. The results confirm that GGBS significantly enhances strength and durability, even at a reduced binder content (400 kg/m³), demonstrating its efficiency in forming a dense, stable, low-permeability matrix. The improvement trends closely mirror those observed in higher-grade mixes (e.g., M50), though the lower total binder mass moderates the overall magnitude of strength and durability gains.

- *Compressive strength:* The compressive strength of M35 mixes rose from 28.8 MPa (control) to 41.6 MPa (100% GGBS) after 28 days, showing calcium oxide (CaO) in GGBS promotes gels that densify the matrix and reduce pore connectivity. GGBS's high reactivity enables rapid geopolymerization at ambient conditions, yielding sufficient strength without heat curing. These findings align with studies by Puertas et al. (2011) and Bernal et al. (2014), indicating that M35-grade concrete can achieve adequate strength with less cement, supporting sustainable design.
- *Flexural and split tensile strength:* Flexural and split tensile strength improved with higher GGBS replacement. 28-day flexural strength increased from 3.46 MPa to 4.99 MPa, and split tensile from 1.73 MPa to 2.50 MPa, a 44–45% rise. This is due to a denser microstructure, fewer microcracks, and a stronger ITZ, thanks to GGBS's higher gel content, enhancing crack resistance and stress redistribution. Nath and Sarker (2014) support these findings, showing reduced defects and improved strength with greater GGBS content. For M35-grade concrete, these strengths are suitable for moderate load-bearing elements, indicating that GGBS-based systems can replace OPC concrete even with lower binder doses.
- *Water absorption and sorptivity:* Durability results confirm GGBS's positive impact. Water absorption dropped from 6.05% to 4.07%, and sorptivity from 0.187 mm/min$^{0.5}$ to 0.125

mm/min$^{0.5}$ at 28 days. These reductions indicate GGBS's pore-filling effect and formation of C–A–S–H gels, which block pores and reduce capillary suction. The matrix becomes denser and less permeable, improving durability. Although absorption and sorptivity are slightly higher than in the M50 series due to the lower binder content, the trend of decreasing permeability with increasing GGBS indicates that microstructural refinement is mainly driven by chemical reactivity rather than binder amount. The lower sorptivity in M35 mixes agrees with Gourley and Johnson (2005), who found that GGBS reduces capillary porosity and water-related deterioration.

- *FTIR and Raman spectroscopy:* Both FTIR and Raman spectra verified a gradual shift in the aluminosilicate network toward a Ca-rich C–A–S–H-dominated structure with increasing GGBS content. A shift in the main Si demonstrated this–O–T band from ~1085 cm^{-1} to ~1045 cm^{-1} in the FTIR spectra. The narrowing and sharpening of Si–O–Si peaks in Raman spectra indicated a more ordered gel network.
- *TGA/DTA:* The low total mass loss (12.4%) indicates high thermal stability, with significant weight loss events related to free water removal, dihydroxylation, and minor carbonate loss decomposition.
- *XRD:* A broad, amorphous hump (20–35° 2θ) became more prominent with increased GGBS, while the quartz peak intensity decreased, confirming a greater reaction extent and enhanced binder phase dominance.

In the M35 series, increasing GGBS content improved compressive, flexural, and tensile strengths, as well as durability indices such as water absorption and sorptivity. Even at lower binder doses, GGBS strongly influences microstructure and performance due to its high calcium reactivity, fine particle size, and latent hydraulic properties that accelerate gel formation. The optimal GGBS range for M35-grade geopolymer concrete is 60–80%, balancing strength, workability, and durability. Beyond 80%, gains diminish due to the cost and workability. GGBS-based geopolymer concrete offers a low-carbon alternative to OPC, with high early strength, low permeability, excellent chemical resistance, and reduced creep under ambient curing conditions. Using GGBS, an industrial by-product, also supports the circular economy by reducing waste and virgin material use—summarising observed trends and mechanisms.

SUSTAINABILITY ASSESSMENT OF M35 GRADE GEOPOLYMER CONCRETE INCORPORATING GGBS

- The sustainability evaluation of the M35-grade polymer–geopolymer hybrid composite demonstrates the material's strong potential as an environmentally responsible and recyclable construction material. By integrating Ground Granulated Blast Furnace Slag (GGBS) into an inorganic polymer matrix, the system effectively transforms industrial by-products into functional composite constituents, thereby minimising waste and resource consumption. This hybrid material not only reduces dependency on energy-intensive Ordinary Portland Cement (OPC) but also exemplifies the principles of circular economy and material valorisation within the construction sector.
- In conventional cementitious systems, OPC production contributes approximately 850–900 kg of CO_2 per ton, with about 60% of these emissions originating from limestone calcination and the remainder from fossil-fuel combustion during clinker production. In contrast, GGBS-based polymer composites exhibit a drastically reduced carbon footprint, as GGBS requires only drying, grinding, and transport prior to use, resulting in emissions of merely 60–80 kg CO_2 per ton. The polymer–geopolymer composite system thus enables significant substitution of high-emission cementitious binders with low-carbon, reactive aluminosilicate materials.
- In this study, the control M35 mix (G1), comprising 100% OPC as the binder, produced an estimated 340–360 kg of CO_2 per cubic meter of concrete. The progressive incorporation of GGBS as a reactive filler within the geopolymeric matrix substantially reduced the embodied carbon. The fully GGBS-based hybrid mix (G6) emitted only 25–35 kg CO_2 per m^3, representing nearly a 90% reduction in embodied emissions. Intermediate substitution levels (60–80% GGBS)

achieved 50–70% reductions in carbon, demonstrating a scalable pathway to producing low-carbon concrete composites.

- Beyond carbon reduction, the polymer–geopolymer hybrid network exhibits intrinsic sustainability advantages, including recyclability, thermal stability, and extended service life. Unlike organic polymer composites, which may degrade thermally or chemically, inorganic polymer matrices maintain structural integrity under high temperatures and chemically aggressive environments. This thermal and chemical resilience translates into longer service life and reduced maintenance requirements, thereby lowering life-cycle energy demand. Additionally, at the end of life, geopolymer composites can be mechanically crushed and reintroduced as a reactive filler or recycled aggregate, enabling partial closed-loop recycling without significant degradation of performance properties.
- The use of GGBS as a key reactive mineral further supports industrial symbiosis, where waste streams from steel manufacturing are redirected into the construction materials sector. This reduces landfill pressure, conserves virgin raw materials, and improves the composite's environmental profile. Moreover, the energy consumption during polymer–geopolymer binder synthesis is significantly lower than that for OPC production, as the process avoids high-temperature clinkerization.

CONCLUSION

This study thoroughly assessed the mechanical, durability, microstructure, and sustainability performance of M35-grade geopolymer concrete with different amounts of Ground Granulated Blast Furnace Slag (GGBS) under ambient curing conditions.

- The results confirmed that increasing GGBS content significantly enhances compressive, flexural, and split tensile strengths, with 28-day compressive strength rising from 28.8 MPa to 41.6 MPa as GGBS increased from 0% to 100%.
- Corresponding reductions in water absorption and sorptivity demonstrated improved pore refinement and reduced permeability. At the same time, FTIR, Raman, TGA/DTA, and XRD analyses validated the formation of a dense, C–A–S–H–dominated gel structure with enhanced matrix stability. From a sustainability perspective, replacing OPC with GGBS led to substantial reductions in embodied carbon—up to nearly 90% at complete replacement—highlighting its potential as a low-carbon binder for structural applications.
- Despite these promising outcomes, certain limitations remain. The investigation was conducted at laboratory scale under controlled ambient curing; therefore, field-scale studies are required to validate performance under variable temperature, humidity, and real environmental exposures.
- The durability assessment, though comprehensive for water transport properties, did not include long-term evaluations such as chloride diffusion over extended periods, carbonation depth, freeze–thaw resistance, and acid/sulfate attack. Additionally, only one activator-to-binder ratio and molarity range were considered, leaving potential optimisation unexplored.
- Future research should focus on long-term field validation of GGBS-based geopolymer concrete in diverse climatic and loading conditions.
- Expanding durability studies to include aggressive chemical exposures, thermal cycling, and reinforcement corrosion behaviour will provide deeper insights into service-life performance.
- There is also scope to explore alternative activator combinations, hybrid precursor systems, and admixture optimisation to enhance workability further, setting behaviour, and early-age strength. Integrating machine learning models for predictive performance assessment and carbon footprint optimisation may support the development of intelligent, data-driven mix design frameworks.

Overall, continued research will strengthen the practical applicability of GGBS-based geopolymer concrete as a sustainable, low-carbon alternative to conventional OPC systems.

REFERENCES

1. Li, C., Pradhan, P., Chen, G. et al. The carbon footprint of the construction sector is projected to double globally by 2050. Commun Earth Environ **6**, 831 (2025). https://doi.org/10.1038/s43247-025-02840-x
2. Nazar, S., Iqbal, M., Yang, J., & Ashraf, M. (2025). Machine Learning-Driven Evaluation of Carbon Emissions in Geopolymer Concrete. Applied Soft Computing, 114017. https://doi.org/10.1016/j.asoc.2025.114017
3. Roviello, G., Occhicone, A., De Gregorio, E., Ricciotti, L., Cioffi, R., Ferone, C., & Tarallo, O. (2025). Geopolymer-based composite and hybrid materials: The synergistic interaction between components. Sustainable Materials and Technologies, e01404. https://doi.org/10.1016/j.susmat.2025.e01404
4. Wu, Y., Lu, B., Bai, T., Wang, H., Du, F., Zhang, Y., ... & Wang, W. (2019). Geopolymer, green alkali-activated cementitious material: Synthesis, applications and challenges. Construction and Building Materials, 224, 930-949.
5. Cong, P., & Cheng, Y. (2021). Advances in Geopolymer Materials: A Comprehensive Review. Journal of Traffic and Transportation Engineering (English Edition), 8(3), 283-314.
6. Kan, L., Chen, B., & Gan, Y. (2025). Engineered geopolymer composites for concrete repair: Durability behaviour and mechanistic investigation under sulfate wet-dry cycles. Journal of Building Engineering, 114323. https://doi.org/10.1016/j.jobe.2025.114323
7. Labaran, Y. H., Mathur, V. S., Muhammad, S. U., & Musa, A. A. (2022). Carbon footprint management: A review of the construction industry. Cleaner Engineering and Technology, 9, 100531. https://doi.org/10.1016/j.clet.2022.100531
8. Sbahieh, S., McKay, G., Nurdiawati, A., & Al-Ghamdi, S. G. (2025). The sustainability of partial and total replacement of Ordinary Portland Cement: A deep dive into different concrete mixtures through life cycle assessment. Journal of Building Engineering, 112830. https://doi.org/10.1016/j.jobe.2025.112830
9. Kanagaraj, B., Anand, N., Raj, R. S., & Lubloy, E. (2023). Techno-socio-economic aspects of Portland cement, geopolymer, and limestone calcined clay cement (LC3) composite systems: a state-of-the-art review. Construction and Building Materials, 398, 132484.https://doi.org/10.1016/j.conbuildmat.2023.132484
10. Adnan, Anas, M. Geopolymer concrete as a sustainable alternative to OPC. J. Umm Al-Qura Univ. Eng. Archit. (2025). https://doi.org/10.1007/s43995-025-00155-8
11. Ayarkwa, J., Opoku, D. G. J., Antwi-Afari, P., & Li, R. Y. M. (2022). Sustainable building processes' challenges and strategies: The relatively necessary index approach. Cleaner Engineering and Technology, 7, 100455. https://doi.org/10.1016/j.clet.2022.100455
12. Firoozi, A. A., Oyejobi, D. O., & Firoozi, A. A. (2025). Innovations in energy-efficient construction: Pioneering sustainable building practices. Cleaner Engineering and Technology, 100957. https://doi.org/10.1016/j.clet.2025.100957
13. Singh, N. B., & Middendorf, B. (2020). Geopolymers as an alternative to Portland cement: An overview. Construction and Building Materials, 237, 117455.
14. Madirisha, M. M., Dada, O. R., & Ikotun, B. D. (2024). Chemical fundamentals of geopolymers in sustainable construction. Materials Today Sustainability, 27, 100842 https://doi.org/10.1016/j.mtsust.2024.100842
15. Amran, M., Al-Fakih, A., Chu, S. H., Fediuk, R., Haruna, S., Azevedo, A., & Vatin, N. (2021). Long-term durability properties of geopolymer concrete: An in-depth review. Case Studies in Construction Materials, 15, e00661.
16. Hakeem, I. Y., Zaid, O., Arbili, M. M., Alyami, M., Alhamami, A., & Alharthai, M. (2024). A state-of-the-art review of the physical and durability characteristics and microstructure behaviour of ultra-high-performance geopolymer concrete. Heliyon, 10(2).
17. Walkley, B., San Nicolas, R., Sani, M. A., Rees, G. J., Hanna, J. V., van Deventer, J. S., & Provis, J. L. (2016). Phase evolution of C-(N)-ASH/NASH gel blends investigated via alkali-activation of

synthetic calcium aluminosilicate precursors. Cement and Concrete Research, 89, 120-135. DOI: 10.1016/j.cemconres.2016.08.010
18. Nasir, M., Mahmood, A. H., & Bahraq, A. A. (2024). History, recent progress, and future challenges of alkali-activated binders–An overview. Construction and Building Materials, 426, 136141. https://doi.org/10.1016/j.conbuildmat.2024.136141
19. Akhtar, N., Ahmad, T., Husain, D., Majdi, A., Alam, M. T., Husain, N., & Wayal, A. K. S. (2022). Ecological Footprint and Economic Assessment of Conventional and Geopolymer Concrete for Sustainable Construction Journal of Cleaner Production, 380, 134910.
20. Mohan Kumar, S. G. K., Kinuthia, J. M., Oti, J., & Adeleke, B. O. (2025). Geopolymer Chemistry and Composition: A Comprehensive Review of Synthesis, Reaction Mechanisms, and Material Properties—Oriented with Sustainable Construction. Materials, 18(16), 3823. https://doi.org/10.3390/ma18163823
21. Salim, M.U., Moro, C. Microstructural insights of geopolymer mortar containing chemosphere: effects on fresh properties and durability. Mater Struct 58, 101 (2025). https://doi.org/10.1617/s11527-025-02636-7
22. Patil, M., Boraste, S., & Minde, P. (2022). A comprehensive review of emerging trends in innovative green building technologies and sustainable materials. Materials Today: Proceedings, 65, 1813-1822.
23. Munro, D., Di Benedetto, G., Graham, M., Jans-Singh, M., Turpin, M., & Kanavaris, F. (2025, August). The assessment of the embodied carbon of resource-constrained materials, including ground granulated blast-furnace slag (GGBS) and ferrous scrap. In Structures (Vol. 78, p. 109175). Elsevier. https://doi.org/10.1016/j.istruc.2025.109175
24. Murali, G. (2024). Recent research in mechanical properties of geopolymer-based ultra-high-performance concrete: A review. Defence Technology, 32, 67-88. https://doi.org/10.1016/j.dt.2023.07.003
25. Davidovits, J. (1991). Geopolymers: Inorganic polymeric new materials. Journal of Thermal Analysis, 37(8), 1633–1656. https://doi.org/10.1007/BF01912193
26. Duxson, P., Fernández-Jiménez, A., Provis, J. L., Lukey, G. C., Palomo, A., & van Deventer, J. S. J. (2007). Geopolymer technology: The current state of the art. Journal of Materials Science, 42(9), 2917–2933. https://doi.org/10.1007/s10853-006-0637-z
27. Duxson, P., Fernández-Jiménez, A., Provis, J. L., Lukey, G. C., Palomo, A., & van Deventer, J. S. J. (2007). Geopolymer technology: The current state of the art. Journal of Materials Science, 42(9), 2917–2933. https://doi.org/10.1007/s10853-006-0637-z
28. Nath, P., & Sarker, P. K. (2014). Effect of GGBFS on setting, workability, and early-strength properties of fly ash geopolymer concrete cured under ambient conditions. Construction and Building Materials, 66, 163–171. https://doi.org/10.1016/j.conbuildmat.2014.05.080
29. Olivia, M., & Nikraz, H. (2012). Properties of Fly Ash Geopolymer Concrete Designed by the Taguchi Method. Materials & Design, 36, 191–198. https://doi.org/10.1016/j.matdes.2011.10.036
30. Gourley, J. T., & Johnson, G. B. (2005). Developments in geopolymer precast concrete. In Proceedings of the International Workshop on Geopolymer Cement and Concrete (pp. 139–149). Perth, Australia: Curtin University of Technology.
31. Patankar, S. V., Jamkar, S. S., & Ghugal, Y. M. (2015). Effect of concentration of sodium hydroxide and degree of heat curing on fly ash-based geopolymer mortar. Indian Journal of Materials Science, 2015, 1–8. https://doi.org/10.1155/2015/852763
32. Aliabdo, A. A., Abd Elmoaty, M., & Salem, H. (2016). Effect of alkali silicate and aluminate modifiers on alkali-activated slag pastes and mortars. Construction and Building Materials, 102, 997–1006. https://doi.org/10.1016/j.conbuildmat.2015.11.021
33. Hewayde, E., Nehdi, M., Allouche, E., & Nakhla, G. (2006). Effect of geopolymer cement on microstructure, compressive strength and sulphuric acid resistance of concrete. Magazine of Concrete Research, 58(5), 321-331.

34. Bouaissi, A., Li, L. Y., Abdullah, M. M. A. B., & Bui, Q. B. (2019). Mechanical properties and microstructure analysis of FA-GGBS-HMNS-based geopolymer concrete. Construction and Building Materials, 210, 198-209. https://doi.org/10.1016/j.conbuildmat.2019.03.202
35. Bellum, R. R., Muniraj, K., & Madduru, S. R. C. (2020). Influence of Activator Solution on the Microstructural and Mechanical Properties of Geopolymer Concrete. Materialia, 10, 100659.
36. Caballero, L. R., Paiva, M. D. D. M., Fairbairn, E. D. M. R., & Toledo Filho, R. D. (2019). Thermal, mechanical, and microstructural analysis of metakaolin-based geopolymers. Materials Research, 22(02), e20180716.
37. Thakur, I. C., Kisku, N., Singh, J. P., & Kumar, S. (2016). Properties of concrete incorporated with GGBS. International Journal of Research in Engineering and Technology, 5(08), 275-281.
38. Yaolin Yi, Martin Liska, Abir Al-Tabbaa; Properties and microstructure of GGBS–magnesia pastes. Advances in Cement Research 1 April 2014; 26 (2): 114–122. https://doi.org/10.1680/adcr.13.00005
39. Xie, J., Wang, J., Rao, R., Wang, C., & Fang, C. (2019). Effects of combined usage of GGBS and fly ash on workability and mechanical properties of alkali-activated geopolymer concrete with recycled aggregate. Composites Part B: Engineering, 164, 179-190.
40. Phoo-Ngernkham, T., Hanjitsuwan, S., Damrongwiriyanupap, N., & Chindaprasirt, P. (2017). Effect of sodium hydroxide and sodium silicate solutions on the strengths of alkali-activated high calcium fly ash containing Portland cement. KSCE Journal of Civil Engineering, 21(6), 2202-2210.
41. Kwek, S. Y., Awang, H., & Cheah, C. B. (2021). Influence of liquid-to-solid and alkaline activator (Sodium silicate to sodium hydroxide) ratios on fresh and hardened properties of alkali-activated palm oil fuel ash geopolymer. Materials, 14(15), 4253.
42. Cheah, C. B., Chow, W. K., Oo, C. W., & Leow, K. H. (2020). The influence of type and combination of polycarboxylate ether superplasticiser on the mechanical properties and microstructure of slag-silica fume ternary blended self-consolidating concrete—Journal of Building Engineering, 31, 101412.
43. Bureau of Indian Standards. (1991). IS 1489 (Part 1): Portland pozzolana cement Specification – Part 1: Fly ash based. New Delhi: Bureau of Indian Standards. https://archive.org/details/gov.in.is.1489.1.1991
44. ASTM International. (2019). ASTM C192/C192M-19: Standard practice for making and curing concrete test specimens in the laboratory. ASTM International. https://doi.org/10.1520/C0192_C0192M-19
45. Bureau of Indian Standards. (1959). IS 1199:1959 – Methods of sampling and analysis of concrete—Bureau of Indian Standards.
46. Bureau of Indian Standards. (2018). IS 516:2018 – Methods of tests for strength of concrete—Bureau of Indian Standards.
47. Bureau of Indian Standards. (1999). IS 5816:1999 – Splitting tensile strength of concrete – Method of test—Bureau of Indian Standards.
48. ASTM International. (2013). ASTM C642-13: Standard test method for density, absorption, and voids in hardened concrete. ASTM International. https://doi.org/10.1520/C0642-13
49. ASTM International. (2018). ASTM C1585-18: Standard test method for measurement of rate of absorption of water by hydraulic-cement concretes. ASTM International. https://doi.org/10.1520/C1585-18
50. ASTM International. (2014). ASTM C1260-14: Standard test method for potential alkali reactivity of aggregates (mortar-bar method). ASTM International. https://doi.org/10.1520/C1260-14

